Temperature dependence of the phosphorescence quantum yield of various α-lactalbumins and of hen egg-white lysozyme

Coleman A. Smith and August H. Maki
Department of Chemistry, University of California, Davis, California 95616 USA

ABSTRACT The radiative quantum yield, Φ_p^o, of the triplet state of human α-lactalbumin (HLA) has been measured in the temperature range between 6 K and the softening point of the aqueous glass (~150 K). Φ_p^o has little temperature dependence below ~30 K, but above this it decreases sharply with increasing temperature. The unusual temperature dependence is fitted by a phenomenological two-state model in which the phosphorescence originates primarily from a donor, tryptophan (Trp) 104, and an acceptor, Trp 60, the populations of which are coupled by a thermally activated triplet–triplet energy transfer process. The model assumes that the acceptor (Trp 60) triplet state undergoes radiationless deactivation by a proximal disulfide residue, while the donor (Trp 104) has no such extrinsic quencher. The decrease of Φ_p^o with increasing temperature is accounted for by the thermally activated triplet–triplet energy transfer process. The disulfide quenching rate constant itself is assumed to be temperature independent, in accord with recent measurements of simple disulfide quenching in long chain snake venom neurotoxins (Schlyer, B. D., E. Lau, and A. H. Maki. 1992. *Biochemistry*. 31:4375–4383; Li, Z., A. Bruce, and W. C. Galley. 1992. *Biophys. J.* 61:1364–1371). We find that the phosphorescence quenching in HLA occurs with an activation energy of 97 cm^{-1}, which we associate with a barrier to the energy transfer process. The data are fit well by the model if we assume a value for the temperature-independent disulfide quenching constant of $k_Q > 3\ s^{-1}$ that is consistent with recent measurements on indole-disulfide model systems (Li, Z., A. Bruce, and W. C. Galley. 1992. *Biophys. J.* 61:1364–1371). Similar results are reported for bovine α-lactalbumin (BLA) and for hen egg-white lysozyme (HEWL) that contains the structural equivalents of Trp 104 and Trp 60 of HLA. HLA provides the best agreement with calculations since it is the simplest, lacking Trp 26, a residue not considered in the model, that probably contributes significantly to the phosphorescence of BLA, guinea pig α-lactalbumin (GPLA), and HEWL. GPLA, which contains Trp 104 but lacks Trp 60, shows qualitatively less thermally induced phosphorescence quenching than HLA, BLA, and HEWL, thus supporting the postulated quenching model.

INTRODUCTION

The phosphorescence emission from proteins is known to be dominated by the amino acid tryptophan (Trp) when it is present. This is due to its larger extinction coefficient and lower excited singlet state energy relative to tyrosine (Tyr) and phenylalanine (Phe), providing an efficient quenching mechanism for the latter via energy transfer. In fluid media, many factors can be responsible for the quenching of triplet emission, resulting in a low phosphorescence quantum yield and a shortened lifetime. However, in rigid solution at temperatures below the glassing point (~160–200 K), where diffusional quenching and radiationless deactivation of the triplet state become negligible; the only intrinsic local perturber known to cause a decrease in phosphorescence quantum yield of both Trp and Tyr is the disulfide bond. A short-lived component in the Trp phosphorescence decay of hen egg-white lysozyme (HEWL) was observed by Churchich in 1966 (1). In 1967, Cowgill (2) studied fluorescence quenching of Trp and Tyr, both in model disulfide compounds and in the β-thiopropionic acid derivative of ribonuclease-A. A later review by Longworth (3) catalogued many proteins exhibiting shortened phosphorescence lifetimes. Among those containing Trp were HEWL, a number of Bence-Jones proteins (immunoglobulins), and bovine α-lactalbumin (BLA). Each of these proteins is known to contain disulfide bonds in the proximity of tryptophan residues.

Work conducted by von Schütz et al. (4) showed that HEWL phosphorescence has a single exponential decay with a lifetime of 6.3 s at 4.2 K, while at 77 K, the decay was observed to be nonexponential, with lifetime components of 1.36 and 4.07 s. Such temperature-dependent phenomena are rare in proteins, and simple disulfide quenching of tryptophan phosphorescence at cryogenic temperatures is known to be temperature independent. The long-chain snake venom neurotoxins, α-bungarotoxin and α-cobratoxin, display phosphorescence components with reduced lifetimes that arise from the single tryptophan, Trp 29. These decay kinetics are independent of temperature between 4.2 and 150 K. Furthermore, the short-lived components are eliminated when the neighboring disulfide, Cys 30–Cys 34, is reduced, thus establishing the identity of the triplet state quencher (5). The lack of temperature dependence of the phosphorescence kinetics of α-bungarotoxin also has been reported recently by Li et al. (6). Although the anomolous phosphorescence lifetime behavior of HEWL has been investigated extensively, no convincing model has been forthcoming to explain its temperature dependence.

The majority of previous work on the spectroscopy of α-lactalbumins has focused on properties determined through the techniques of fluorescence and nuclear magnetic resonance (NMR). A comprehensive review appeared in 1988, in which Berliner and Johnson (7) discuss calcium binding in α-lactalbumin and calmodulin. In this review, the structural differences of apo- and holo-α-lactalbumin are presented. The holoenzyme

0006-3495/93/06/1885/11 $2.00

structure is known to be similar to HEWL (see discussion below). The dissociation constant for Ca^{2+} in α-lactalbumin is extremely small ($\sim$1–10 nM) (7), so that the spectral contribution from Trps in the apoenzyme structure can be disregarded when the enzyme is calcium loaded (1:1 mol/mol ratio). In 1980 Sommers and Kronman (8) compared the fluorescence of α-lactalbumin from bovine, goat, human (HLA), and guinea pig (GPLA) sources in fluid solution. In this work, the authors conclude that "the energy of excitation is channeled from Trp 26 and 104 to Trp 60 (if present), where it is quenched as a result of the close proximity of the latter residue to the disulfide bridges 73–91 and 61–77."

The direct quenching of Tyr (9) and Trp (10) fluorescence by oxidized dithiothreitol (DTT) in fluid solution has been attributed primarily to a static process, rather than to dynamic collisional quenching. In these studies, the formation of a ground state complex between Tyr or Trp and the disulfide bond of the oxidized DTT was suggested. The strength of this interaction is proposed to be modified by the immediate environment of the chromophore (10). Such a complexation would be expected to be short range in nature, and may account for the singlet level quenching of Trp 60 in α-lactalbumin, due to its proximity to the disulfide bridges 73–91 and 61–77 as suggested by Sommers and Kronman (8).

Triplet state quenching of Trp by disulfide was shown to occur via an electron transfer process by Bent and Hayon in 1974 (11). In their study, L-Trp monomer in aqueous buffer was photoionized with a 265-nm laser pulse in the presence of alkyl disulfide (RSSR)-type compounds. The authors found the occurrence of a reaction of the following type:

$$^3\text{Trp} + \text{RSSR} \rightarrow \text{Trp}\cdot^+ + \text{RSSR}\cdot^-.$$

The quenching mechanism was found to occur, at least in part, by transfer of an electron with the formation of the $\text{RSSR}\cdot^-$ radical anion. In work to be reported below, we find a large decrease in the tryptophan phosphorescence-to-fluorescence quantum yield ratio (Φ_p/Φ_f) of HLA, BLA, and HEWL with increasing temperature, indicating thermally activated quenching of Trp luminescence at the triplet level. One would expect Φ_p/Φ_f to remain constant if all of the luminescence reduction (energy transfer + disulfide quenching) occurred at the singlet level. We will present results suggesting that the rate-determining step in the phosphorescence quenching process of Trp 104 in the α-lactalbumins and Trp 108 in HEWL is thermally activated triplet–triplet energy transfer between Trp residues in these proteins.

The crystal structure of HEWL has been known for many years. The original structure of the tetragonal form was solved by Blake et al. (12) in 1965, at a resolution of 2 Å. A 1.97-Å resolution structure of the triclinic form was solved in 1976 by Kurachi et al. (13). The Kurachi structure was used for calculations in the present study, since these coordinates have been deposited in the Brookhaven Protein Data Bank. HEWL contains six Trps and four disulfide bonds. Lactalbumin, on the other hand, contains either three or four Trps, depending on the species. The same set of four structurally equivalent disulfide bonds found in HEWL is present in all lactalbumins. The structural similarity between HEWL and the lactalbumins has long been recognized, but it was not until 1989 that the crystal structure of baboon α-lactalbumin was solved (14), and the atomic coordinates of the two proteins, α-lactalbumin and HEWL, could be compared directly. It should be noted here that baboon α-lactalbumin is highly homologous to HLA, with all Trps and disulfide bonds strictly conserved. Therefore, for the purposes of this study, these two structures will be considered identical, even though a HLA structure has yet to be solved. The origin of Trp fluorescence in HEWL was investigated in 1971 by Imoto et al. (15) through the use of oxindole-62 and oxindole-108 derivatives. They concluded that Trps 108 and 62 are the source of >80% of the emission from HEWL. Later, phosphorescence and optically detected magnetic resonance (ODMR) studies of these same oxindole derivatives showed that Trp 108 dominates the phosphorescence of HEWL at pumped liquid helium temperatures (16).

The distance dependence of disulfide quenching of Trp phosphorescence was demonstrated in 1989 by Li and Galley (17), who monitored the effect of substrate binding on the phosphorescence lifetime of HEWL at 77 K. The lengthening of the phosphorescence lifetime upon binding of N',N'',N'''-triacetyl chitotriose was attributed to a conformational change in the protein, in which emitting Trps were shifted farther away from a disulfide bond. The distance dependence for the triplet state quenching of an indole derivative by disulfide was studied further by Li et al. (18) using the model compound 2-(3-indolyl)ethyl phenyl ketone (IEPK), in a random distribution with sec-dibutyl disulfide. IEPK was first introduced by Tamaki (19) in 1981, and was chosen as a model compound because excitation energy is channeled very rapidly from the directly excited triplet state of the ketone sensitizer to the indole triplet state, thereby eliminating quenching at the singlet level. Li et al. (18) found that the quenching followed a Dexter-type distance dependence, and calculated quenching constants of 110 and 7.4 s^{-1} for a separation between quencher and chromophore of 2 and 3 Å beyond van der Waals contact, respectively, at 77 K. They found a limiting quenching rate constant of $\sim 2 \times 10^4\ s^{-1}$ at 77 K for the indole triplet state in IEPK with increasing sec-dibutyl disulfide concentration. This quenching constant was interpreted as an upper limit of the triplet decay constant for the indole chromophore in van der Waals contact with disulfide. In a recent study, Li et al. (6) have measured the temperature dependence of the disulfide quenching of IEPK. It was found that the limiting

quenching rate constant (its value at van der Waals contact, according to the quenching model used) increases with temperature >30 K, changing from a constant value of 500 s^{-1} <30 K to ~2.3×10^4 s^{-1} at $T \sim 90$ K. This rate constant is many orders of magnitude smaller than the 10^{10}–10^{12} s^{-1} that would be expected for simple barrier-free electron transfer (20). The temperature dependence in this range appears to correspond to Arrhenius behavior with an activation energy of 190 cm^{-1}, which was attributed to an activation barrier to the disulfide quenching process itself. This interpretation, which does not take into consideration the possibility of triplet–triplet energy transfer among the IEPK donor population, is at variance with the lack of temperature dependence observed (5, 6) in the intramolecular disulfide quenching of α-bungarotoxin and α-cobratoxin where triplet–triplet energy transfer is not possible. The temperature dependence of the disulfide quenching of HEWL phosphorescence was found (6) to be qualitatively similar to that observed in the random IEPK-disulfide model system.

In this work we characterize the phosphorescence quantum yield of α-lactalbumins from several species and of HEWL at temperatures in the range 6–200 K. We will present evidence to show that the phosphorescence quenching of the most luminescent Trp in HLA and BLA (Trp 104) and in HEWL (Trp 108) proceeds via a thermally activated triplet–triplet energy transfer to Trp 60 (Trp 63 in HEWL), the emission of which is quenched with high efficiency by nearby disulfide residues.

MATERIALS AND METHODS

Sample preparation

HEWL was purchased from Schwarz/Mann (Spring Valley, NY) and was used without further purification. BLA and HLA were purchased from Sigma Chemical Co. (St. Louis, MO). GPLA was a generous gift from Dr. Marvin Thompson. All α-lactalbumins were calcium loaded (1:1). The conformation of calcium-bound α-lactalbumin is known to be different from that of the apoprotein (7, 21). Since the apoprotein structure is known not to be isostructural with HEWL, the apo-lactalbumins were not investigated in this study. Each protein was exchanged into a 10-mM potassium phosphate buffer, pH 7.0. A cryosolvent was added before freezing, in order to reduce the possibility of distortion of the protein structure and/or aggregation upon ice formation. Either ethylene glycol (puriss; Fluka AG, Buchs, Switzerland) 30% (vol/vol) or glucose 1% (wt/wt), was added. Reduction in phosphorescence quantum yield has been observed in purely aqueous ices of benzo(a)pyrene tetraol (22). It was postulated that molecular aggregation could be occurring among the monomers, creating favorable conditions for triplet–triplet energy migration. However, in this study, the quantity or type of cryosolvent did not have a significant effect on the phosphorescence quantum yield of any of the proteins studied. Even when the protein was frozen as a purely aqueous ice, there was no indication, either in the location or shape of the spectral peaks, or in the calculated quantum yield, that a distortion of the protein structure occurred. Typical protein concentrations were 1–3 mM.

Experimental

The protein solutions were loaded into small Suprasil (Heraeus Amersil, Inc., Buford, GA) quartz tubes of 2 mm I.D., with a volume of ~40 μl. The samples were then mounted in a copper block holder that serves as a heat sink, and lowered into the optical tail of a dewar (Super-Varitemp; Janis Research Co. Inc., Stoneham, MA). This system, working in conjunction with a temperature controller (model 805; Lake Shore Cryotonics, Inc., Westerville, OH), has the capability of very accurate temperature control (±0.01 K) in the range 3.4–300 K. A calibrated Ge diode sensor was attached directly to the Cu heat sink containing the sample tube. Optical excitation was accomplished via a 450-W high-pressure Xe arc lamp, the output of which passed through a double prism monochromator (model 50-650-000; Cary Instruments, Palo Alto, CA). Excitation of all samples was at 290 nm with 5-nm bandpass. Emission was detected at right angles through a 2/3 m monochromator (model 207; McPherson, Inc., Acton, MA) fitted with a cooled (−20°C) photomultiplier. The emission was typically scanned through the range 295–550 nm using 2.5-nm bandpass. Output from the photomultiplier was digitized by a signal averager (model TN-1550; Tracor Northern, Middleton, WI) and then loaded into a computer (model Step 386/20; Everex Systems, Inc., Fremont, CA) for analysis.

Total luminescence spectra were typically collected with increasing temperature, as temperature equilibration within the cryostat occurred more rapidly. However, studies on each of the four samples revealed identical temperature dependence of the integrated areas of the spectra when collected with decreasing temperature. That is, no hysteresis in the temperature dependence of the quantum yield was observed.

In all cases, the ratio of the phosphorescence-to fluorescence quantum yields was obtained by numerical integration of the total luminescence spectrum, via the software Sigma-Plot (Jandel, Inc., San Rafael, CA). Absolute ratios were obtained by comparison with a 1-mg/ml solution of L-Trp (Fluka microselect) in 1:1 (vol/vol) ethylene glycol/water at 77 K, for which Φ_p/Φ_f is taken to be 0.28 (3, 23). In some cases, there was a small amount of Trp fluorescence underlying the phosphorescence. The magnitude of this underlying fluorescence was estimated by extrapolating the tail of the fluorescence. This correction, when made, never changed the calculated quantum yield ratio by more than a few percent.

The experimental data as a function of temperature were fit to a mathematical expression arising from a quenching model described below. The least-squares best-fit of the data to this expression was performed within Sigma-Plot, which uses a Marquardt-Levenberg algorithm. Required input to this program includes the function, the data file to be fit, and initial guesses for the parameters in the function. Output of this program yields the best-fit parameters and the norm of the fit, defined as the square root of the sum of the squares of the residuals.

THEORETICAL MODEL

The quantity measured in this study is the phosphorescence-to-fluorescence quantum yield ratio, calculated from total luminescence spectra. This ratio, which compensates for temperature-dependent quenching at the singlet level, can be related to a triplet state radiative quantum yield, and may be expressed in the following way. Let Φ_p and Φ_f represent the phosphorescence and fluorescence quantum yields, respectively. Then we may write:

$$\Phi_p = [k_{isc}/(k_Q^f + k_{isc} + k_f)] \cdot \Phi_p^\circ \quad (1)$$

$$\Phi_f = k_f/(k_Q^f + k_{isc} + k_f). \quad (2)$$

Here, k_{isc} is the rate constant for $S_1 \Rightarrow T_1$ intersystem crossing, k_f is the rate constant for fluorescence, and k_Q^f represents the rate constant for external quenching at the singlet level. In Eq. 1, Φ_p° represents the radiative quantum yield of the triplet states that are produced. We may

avoid possible effects of a temperature-dependent k_Q^f by writing the following expression for the temperature-dependent quantum yield ratio:

$$\Phi_p(T)/\Phi_f(T) = [k_{isc}/(k_Q^f + k_{isc} + k_f)] \cdot [(k_Q^f + k_{isc} + k_f)/k_f] \cdot [\Phi_p^\circ(T)] = [k_{isc}(T)/k_f(T)] \cdot [\Phi_p^\circ(T)]. \quad (3)$$

We may write a similar expression for the quantum yield ratio at low temperature, $T \sim 0$, when temperature-dependent external quenching at both the singlet and triplet levels is negligible:

$$\Phi_p(0)/\Phi_f(0) = [k_{isc}(0)/k_f(0)] \cdot [\Phi_p^\circ(0)] \quad (4)$$

Taking the ratio of Eqs. 3 and 4 above, we may write:

$$[\Phi_p(T)/\Phi_f(T)]/[\Phi_p(0)/\Phi_f(0)] = [k_{isc}(T)/k_f(T)] \cdot [k_f(0)/k_{isc}(0)] \cdot [\Phi_p^\circ(T)/\Phi_p^\circ(0)] \cong [\Phi_p^\circ(T)/\Phi_p^\circ(0)]. \quad (5)$$

The final expression above results from the reasonable approximation that the intrinsic fluorescence decay and $S_1 \Rightarrow T_1$ intersystem crossing rates are relatively temperature independent in the range of our measurements.

The temperature dependence of the phosphorescence quantum yield ratio given in Eq. 5 can be modeled using a two-level system. Assume the protein contains two active tryptophan residues connected by triplet–triplet energy transfer. The donor triplet state is assumed to exhibit only intrinsic tryptophan decay kinetics, while the acceptor triplet state additionally undergoes extrinsic quenching by a nearby disulfide. We then define the following quantities for the donor and acceptor triplet states:

$$\Phi_d^\circ(T) = k_d^r/(k_d^r + k_d^{nr}) = k_d^r/k_d \quad (6)$$

$$\Phi_a^\circ(T) = k_a^r/(k_a^r + k_a^{nr} + k_Q) = k_a^r/k_a. \quad (7)$$

Let $N_d^\circ(T)$ and $N_a^\circ(T)$ be the fractions of the total photostationary state triplet population in the donor and acceptor triplet states, respectively. The observed temperature-dependent triplet radiative quantum yield of this model protein is given by

$$\Phi_p^\circ(T) = N_d^\circ(T)\Phi_d^\circ(T) + N_a^\circ(T)\Phi_a^\circ(T). \quad (8)$$

We assume that energy transfer can occur at the triplet level between the donor and acceptor. Following the example of Hall and El-Sayed (24), the kinetics of this system may be expressed as

$$D\mathbf{N}(T) = \mathbf{P} + \mathbf{A}\mathbf{N}(T), \quad (9)$$

where $\mathbf{A}$ is the rate matrix, $\mathbf{N}(T)$ is the temperature-dependent state population column vector with elements $N_d(T)$ and $N_a(T)$, $\mathbf{P}$ is the populating rate vector with elements P_d and P_a, and D is the time-differential operator. The rate matrix is

$$\mathbf{A} = \begin{pmatrix} -(k_d + k_{fet}) & k_{ret} \\ k_{fet} & -(k_a + k_{ret}) \end{pmatrix}, \quad (10)$$

where k_{fet} and k_{ret} are the rate constants for forward and reverse triplet–triplet energy transfer, respectively. Under steady-state excitation, we may write

$$D\mathbf{N}(T) = \mathbf{P} + \mathbf{A}\mathbf{N}^\circ(T) = 0, \quad (11)$$

where $\mathbf{N}^\circ(T)$ is the population vector of the photostationary state, with elements $N_d^\circ(T)$ and $N_a^\circ(T)$. This yields

$$\mathbf{A}\mathbf{N}^\circ(T) = -\mathbf{P}, \quad \text{and} \quad (12)$$

$$\mathbf{A}^{-1}\mathbf{A}\mathbf{N}^\circ(T) = \mathbf{N}^\circ(T) = -\mathbf{A}^{-1}\mathbf{P}. \quad (13)$$

The proposed acceptor, Trp 60 in HLA and Trp 63 in HEWL, is known to lie close to two disulfide bridges (13, 14). When in close proximity, disulfide quenching of Trp is known to be efficient at the singlet level (2, 9, 10). Therefore, we assume that the acceptor singlet state is quenched, yielding values of 1 and 0 for the normalized populating rates of the donor and acceptor triplets, respectively. Thus, from Eq. 13 we obtain

$$N_d^\circ(T) = (k_a + k_{ret})/(k_a k_d + k_a k_{fet} + k_d k_{ret}), \quad \text{and} \quad (14)$$

$$N_a^\circ(T) = k_{fet}/(k_a k_d + k_a k_{fet} + k_d k_{ret}). \quad (15)$$

Upon substitution from Eqs. 14 and 15 into Eq. 8, the triplet radiative quantum yield becomes

$$\Phi_p^\circ(T) = [(k_a + k_{ret})\Phi_d^\circ(T) + k_{fet}\Phi_a^\circ(T)]/(k_a k_d + k_a k_{fet} + k_d k_{ret}). \quad (16)$$

At low temperature, when the temperature-dependent energy transfer process is negligible, we may write the following rate expressions for the donor and acceptor:

$$dN_d(0)/dt = P_d - k_d N_d(0) \quad (17)$$

$$dN_a(0)/dt = P_a - k_a N_a(0). \quad (18)$$

Following the example above, we obtain, in the photostationary state,

$$N_d^\circ(0) = 1/k_d, \quad \text{and} \quad (19)$$

$$N_a^\circ(0) = 0. \quad (20)$$

The assumption that $P_a = 0$ implies $N_a^\circ(0) = 0$, since the acceptor in our model has no populating pathway available in the absence of thermally activated energy transfer. From Eqs. 8, 19, and 20, we obtain

$$\Phi_p^\circ(0) = \Phi_d^\circ(0)/k_d. \quad (21)$$

Taking the ratio of Eqs. 16 and 21 as given in Eq. 5, we get

$$\Phi_p^\circ(T)/\Phi_p^\circ(0) = k_d\Phi_p^\circ(T)/\Phi_d^\circ(0), \quad (22)$$

where $\Phi_p^\circ(T)$ is given by Eq. 16. Assuming that the intrinsic triplet rate constants of the donor and acceptor

TABLE 1 **Positions of Trp residues in HEWL and α-lactalbumin**

HEWL	BLA	HLA	GPLA
W28	W26	(L26)	W26
W62	(I59)	(L59)	(D59)
W63	W60	W60	(F60)
W108	W104	W104	W104
W111	(H107)	(H107)	(H107)
W123	W118	W118	W118

The one-letter standard designations for amino acids are used. HEWL contains 129 amino acids, compared with 123 for the α-lactalbumins. Hence, the numbering schemes presented are different for the two proteins. However, each row in the table represents a structurally equivalent site (12). The four disulfide bonds in HEWL and the α-lactalbumins are structurally conserved. HEWL, hen egg-white lysozyme; BLA, HLA, and GPLA, α-lactalbumins from bovine, human, and guinea pig sources, respectively.

Trp residues are equal, we obtain $k_d = k_o$ and $k_a = k_o + k_Q$. Here, k_Q is an extrinsic quenching rate constant. We assume further that k_o^r and k_o^{nr} are the same for the donor and acceptor and are temperature independent below the glassing temperature. This allows us to write $\Phi_d^o(T) = \Phi_d^o(0)$, and $\Phi_a^o(T) = \Phi_d^o(0)k_o/(k_o + k_Q)$. Then Eq. 22 simplifies to

$$[\Phi_p^o(T)/\Phi_p^o(0)] = \{k_Q + k_o + k_{ret} + [k_o k_{fet}/(k_o + k_Q)]\}/ \{k_Q + k_o + k_{ret} + [(k_o + k_Q)k_{fet}/k_o]\}. \quad (23)$$

We now adopt a model in which the donor and acceptor states communicate via a reversible thermally activated mechanism. The forward and reverse energy transfer rates then may be expressed as

$$k_{fet} = k_{fet}^{\infty} \cdot \exp(-\Delta E_f/kT) \quad (24)$$

$$k_{ret} = k_{ret}^{\infty} \cdot \exp(-\Delta E_r/kT), \quad (25)$$

where ΔE_f and ΔE_r are activation energies associated with the forward and reverse energy transfer processes, respectively, and k is the Boltzmann constant. The preexponentials for the forward and reverse transfer are expressed as k_{fet}^{∞} and k_{ret}^{∞}, respectively. These preexponential terms are interpreted as the limiting high-temperature energy transfer rate constants. It is reasonable to assume that the forward and reverse rate constants are equal in the limit of high temperature, so we now introduce $k_{tr} = k_{fet}^{\infty} = k_{ret}^{\infty}$. Substituting into Eq. 23, we obtain

$$[\Phi_p^o(T)/\Phi_p^o(0)] = [A/(1 - B) + \exp(-\Delta E_r/kT) + B\exp(-\Delta E_f/kT)]/ [A/(1 - B) + \exp(-\Delta E_r/kT) + (1/B)\exp(-\Delta E_f/kT)], \quad (26)$$

where $A \equiv k_Q/k_{tr}$ and $B \equiv k_o/(k_o + k_Q)$. Henceforth, the left side of Eq. 26 as well as the left side of Eq. 5 will be referred to simply as $f(T)$, and will appear as the label of the ordinate in all subsequent plots that refer to this model.

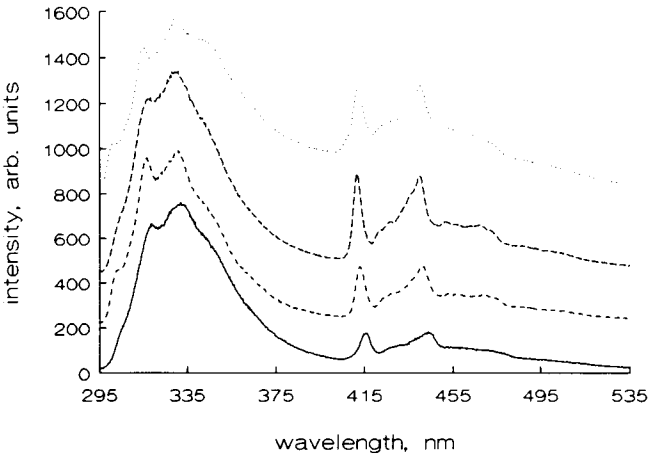

FIGURE 1 The total luminescence spectra of the four proteins studied. Symbols are as follows: HEWL, ——; BLA, - - - - -; HLA, — —; GPLA, · · · ·. Excitation was at 290 nm, 5-nm bandpass, via a 450-W high-pressure Xe arc lamp and a double-prism monochromator. Emission was detected through a 2/3-m monochromator with a 2.5-nm bandpass. Sample temperature was 6 K. Conditions were identical for all samples.

RESULTS

The number and positions of all Trps in HEWL and the α-lactalbumins are given in Table 1. It can be seen that HEWL and BLA contain the highest number of Trps other than the $d \Rightarrow a$ pair assumed to be involved in energy transfer. Fig. 1 shows the total luminescence spectra of each of the four proteins at 6 K. One may notice visually that Φ_p/Φ_f at 6 K is smallest for HEWL compared with the lactalbumins, suggesting that more of the phosphorescence in this protein may be quenched in a temperature-independent process. This is also true of BLA compared with HLA. The proximity of disulfide bonds to the Trps not involved in energy transfer might lead one to expect the direct disulfide quenching of Trp phosphorescence to be greatest for those proteins. Table 2 lists the phosphorescence 0–0 band wavelengths and energies for each of the four proteins shown in Fig. 1. Although no spectra are shown for the higher temperatures, no significant temperature-dependent spectral

TABLE 2 **0–0 Band wavelengths and energies**

Species	λ_{0-0}*	ν_{0-0}
	nm	cm^{-1}
HEWL	414.1	24,140
BLA	414.6	24,110
HLA	411.9	24,270
GPLA	411.7	24,280

* The 0–0 band is assumed to arise primarily from Trp 108 phosphorescence emission in HEWL and Trp 104 emission in the α-lactalbumins. Abbreviations, see Table 1.

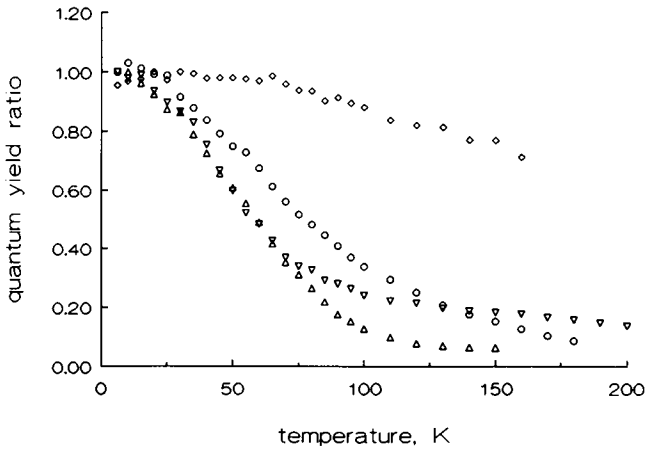

FIGURE 2 A plot of the experimental quantity $\{[\Phi_p(T)/\Phi_f(T)]/[\Phi_p(0)/\Phi_f(0)]\}$ as a function of temperature, showing data in the range 6 K to the approximate glassing point ($\sim$160–200 K) for each of the four proteins. The following symbols are used: Δ, HEWL; O, BLA; ∇, HLA; and ◇, GPLA. Each data point represents a calculated phosphorescence-to-fluorescence quantum yield ratio (Φ_p/Φ_f) from spectra similar to Fig. 3, and corrected for instrumental factors as described in the text.

shifts of the phosphorescence 0–0 bands were observed for any of the four proteins studied.

Fig. 2 shows the temperature dependence of $\{[\Phi_p(T)/\Phi_f(T)]/[\Phi_p(0)/\Phi_f(0)]\} \equiv f(T)$ for each of the four proteins studied. Data were taken at 5-K intervals from 10 through 100 K, and at 10-K intervals from 100 K to the approximate glassing temperature. An additional data point was taken at 6 K, the lowest temperature reasonably attainable without immersing the sample in liquid helium. The glassing temperature varied slightly with the sample, but was estimated to be in the range 160–200 K, as evidenced by a sudden sharp decrease in Φ_p/Φ_f.

We attempted, initially, to fit our data from HLA to Eq. 26 in order to determine the four parameters. It should be mentioned at the outset that none of the proteins investigated in this work can be considered an ideal example of the adopted model in that Trp residues are present in addition to the postulated donor–acceptor pair. Thus, to the extent that these Trps contribute to the phosphorescence, it would be unreasonable to expect quantitative agreement with the model. HLA was chosen for initial analysis since it contains only one Trp residue (Trp 118) in addition to the proposed energy transfer pair, Trps 104 and 60. Trp 118 is quite close to the disulfide Cys 28–Cys 111, and may be largely quenched at the singlet level (2, 9, 10). Therefore, we anticipate that HLA should represent the most faithful protein representative of the triplet–triplet energy transfer model adopted in this paper. It became apparent that the parameters ΔE_f, ΔE_r, k_{tr}, and k_Q are heavily linked and cannot be determined uniquely. The intrinsic decay constant, k_o, is not considered to be an independent variable; it is obtained from the measured phosphorescence decay kinetics at $T = 6$ K, which yield $k_o = 0.16\ s^{-1}$. Since all parameters cannot be obtained uniquely from the data analysis, we sought reasonable limits for some of them. Since k_Q has been found to be temperature independent (5, 6), we assume that k_Q is constant with a value in the range $1–100\ s^{-1}$ for HLA. Values of k_Q below this range fit the data poorly while for $k_Q > 10\ s^{-1}$ the agreement becomes insensitive to its magnitude. See discussion below. ΔE_f and ΔE_r are related by the difference in the triplet state electronic energy of the donor and acceptor residues. The energy of the donor triplet state can be obtained from λ_{0-0} observed at low temperature. The λ_{0-0} are given in Table 2 for each protein that was studied. The low-temeprature λ_{0-0} for HLA, which is found at 411.9 nm, is characteristic of a moderately polarizable local environment (25). The λ_{0-0} of the trap site, Trp 60, cannot be determined directly, since emission from this residue is largely quenched. However, the environment of Trp 60 should be quite polarizable because of the nearby disulfide residues. Phosphorescence has been observed from a Trp residue in glyceraldehyde-3-phosphate dehydrogenase with $\lambda_{0-0} = 420$ nm (26). Recently (27, 28), the binding of an arsenic atom in the neighborhood of a Trp site in EcoRI methylase has been found to induce a red shift of λ_{0-0} from 412.3 to 420.5 nm. Such red shifts probably are extreme, but they provide a reasonable estimate for the maximum trap depth in HLA, leading to $\Delta E/k(\max) = 660$ K. ΔE_f is determined quite well by the low-temperature data points, and is relatively insensitive to the values of the other parameters for fits that produce low norms (see below). Good fits invariably produced $\Delta E_f/k \sim 140$ K. We have made a series of least-squares fits of our HLA data to Eq. 26, using a range of fixed values for k_Q and ΔE_r. k_Q was varied between 0.3 and $100\ s^{-1}$, while $\Delta E_r/k$ was fixed at either 140 K (corresponding to an acceptor residue at roughly the same energy as the donor) or 800 K (corresponding to a trap that probably has the maximum reasonable depth, and is consistent with $\lambda_{0-0} = 420$ nm). The results are presented in Table 3. Certain features emerge from examining the results. Small values of k_Q fit the data poorly, as judged from the norms. $k_Q \gtrsim 3\ s^{-1}$ is required to produce a reasonable fit for either value of ΔE_r. For larger values of k_Q, the best values of ΔE_f and k_{tr} become relatively insensitive to either k_Q or ΔE_r, as does the norm for the fit. To illustrate the inadequacy of a small value of k_Q for fitting the data, we show in Fig. 3 the best fit of the HLA data to Eq. 26 for $k_Q = 0.3\ s^{-1}$ and $\Delta E_r/k = 800$ K. The data are fitted quite poorly, particularly in the high-temperature region, and the norm is relatively large. A shallower trap produces an even poorer fit of the data for this assumed value of k_Q (Table 3). If k_Q is increased to $10\ s^{-1}$, the fit is considerably improved, as can be seen in Fig. 4. If k_Q is increased further above $10\ s^{-1}$, equally good fits are obtained. Also, the goodness of the fit be-

TABLE 3 **Trial fits of f(T) to HLA for various values of k_Q and $\Delta E_r/k$**

k_Q*	$\Delta E_r/k$*	$\Delta E_f/k$‡	k_{tr}‡	Norm§
s^{-1}	K	K	s^{-1}	
0.3	140	128.9	4.603	0.7524
0.3	800	182.3	5.505	0.1681
1	140	191.6	9.074	0.2039
1	800	145.2	2.190	0.1072
3	140	154.7	2.722	0.1159
3	800	140.7	1.942	0.1040
10	140	143.8	2.087	0.1060
10	800	140.0	1.907	0.1037
30	140	141.2	1.960	0.1043
30	800	139.9	1.902	0.1037
100	140	140.2	1.897	0.1039
100	800	139.9	1.880	0.1037

HLA, human α-lactalbumin. *The parameters k_Q and $\Delta E_r/k$ were fixed at these values. ‡The parameters $\Delta E_f/k$ and k_{tr} were fit by a nonlinear least-squares algorithm. §The norm of the fit is defined as the square root of the sum of the squares of the residuals.

comes insensitive to ΔE_r. Thus, it is apparent that k_Q and ΔE_r are determined very poorly above certain lower limits, and therefore we will adopt certain reasonable values in the analysis of the data. For k_Q, we adopt 10 s^{-1} (see discussion below), based on the work of Li et al. (6, 18), and for $\Delta E_r/k$ we have used 800 K, although, as mentioned above, for this value of k_Q the results are insensitive to the trap depth.

Using these assumed values, the least-squares best fits of our data for HLA, BLA, and HEWL are given in Figs. 4, 5, and 6, respectively. The qualitatively different data for GPLA are shown in Fig. 7 for comparison, but no attempt to fit these data was made since this protein lacks Trp 60, and should not be fit by this quenching model. The least-squares best-fit parameters, ΔE_f and

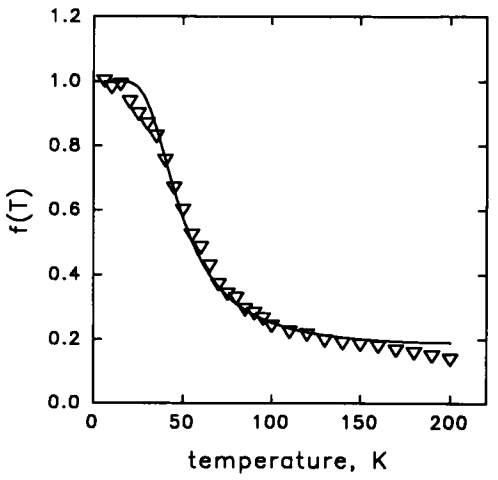

FIGURE 3 A best-fit plot of f(T) to the experimental data from HLA, with the following parameters fixed: k_Q = 0.3 s^{-1} and $\Delta E_r/k$ = 800 K. This figure illustrates the inability of the model to fit the data when k_Q approaches k_o = 0.16 s^{-1}, especially in the high-temperature region.

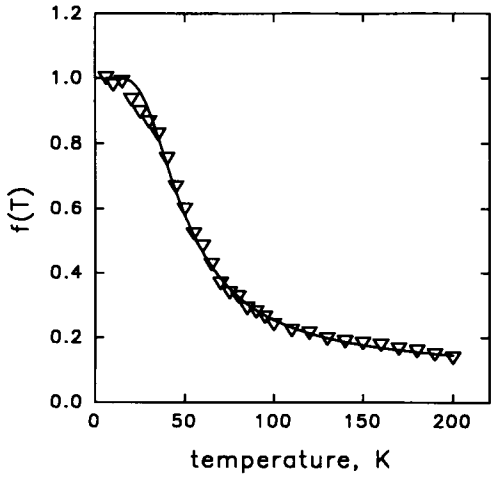

FIGURE 4 A nonlinear least-squares fit of the experimental data from HLA to the function f(T). The data were plotted as $\{[\Phi_p(T)/\Phi_f(T)]/[\Phi_p(0)/\Phi_f(0)]\}$ vs. T, as described in Fig. 3. The analysis yielded ΔE_f = 97.2 cm^{-1} and k_{tr} = 1.91 s^{-1}. For this and all subsequent fits of other samples, we assumed the values $\Delta E_r/k$ = 800 K and k_Q = 10 s^{-1} (see text).

k_{tr}, for HLA, BLA, and HEWL are given in Table 4. The poorer fits of BLA and HEWL to our model are apparent from the norms produced by the fit, as well as from comparison of Figs. 4–6. The reason for the expected poorer fit of the BLA and HEWL data probably arises from the contribution of Trp phosphorescence emission that is not accounted for by the proposed minimalistic two-level system model. This is suggested, also, by differences in λ_{0-0} between HLA and the two other proteins, HEWL and BLA (Table 2).

DISCUSSION

The work of Li et al. (6, 17, 18) on the disulfide quenching of the tryptophan triplet state represents the most

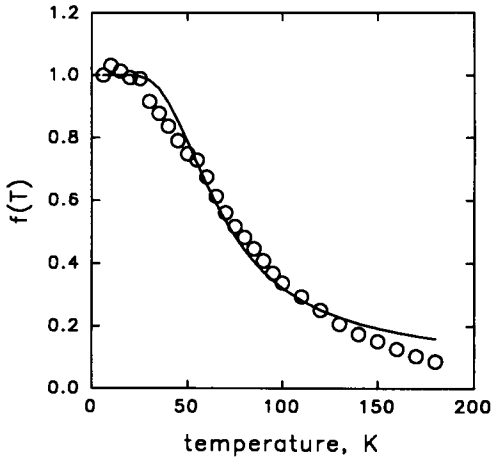

FIGURE 5 A least-squares fit of the data from BLA to f(T). The analysis yielded ΔE_f = 143 cm^{-1} and k_{tr} = 2.66 s^{-1}. The values $\Delta E_r/k$ = 800 K and k_Q = 10 s^{-1} were assumed.

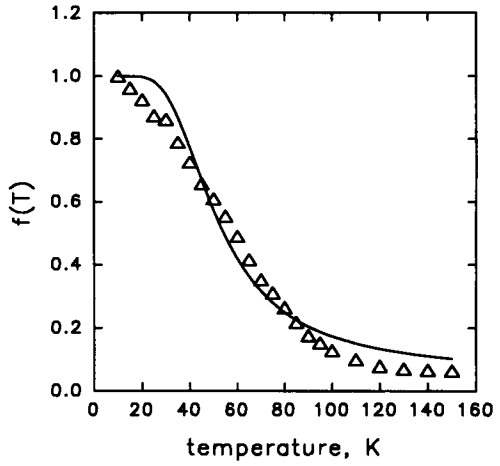

FIGURE 6 A least-squares fit of the data from HEWL to f(T). The analysis yielded ΔE_f = 130 cm^{-1} and k_{tr} = 4.95 s^{-1}. The values $\Delta E_r/k$ = 800 K and k_Q = 10 s^{-1} were assumed.

thorough investigation to date of this phenomenon. Recent studies (6) of the temperature dependence of the disulfide quenching rate constant of the IEPK–disulfide model system, however, are at variance with the earlier suggestion (18) that the quenching occurs by an endothermic triplet–triplet energy transfer to disulfide. The observed activation energy of 190 cm^{-1} (6) is too small to be consistent with this idea, and quenching by the electron transfer mechanism (11) is suggested. The temperature dependence of the observed quenching constant in the IEPK-disulfide system cannot be attributed to the quenching step, itself, in our view, since the Trp phosphorescence quenching by cystine in α-bungarotoxin (5, 6) and α-cobratoxin (5) is known to be independent of temperature. These toxins are simpler systems, containing only one Trp residue located in the vicinity of a single disulfide quencher. Although the source of the temperature dependence of quenching in the IEPK-disulfide system has not been clearly defined, one distinct possibility that should be considered is that thermally activated triplet–triplet energy transfer among the randomly dispersed indole residues is a factor in the quenching mechanism. It is significant, we think, that the activation energy of 190 cm^{-1} obtained in the work of Li et al. (6) is similar to the values of ΔE_f that we find in our protein measurements (Table 4). If energy transfer does contribute to the quenching mechanism in Li et al.'s model system (6, 18), the data at elevated temperatures, $T > 30$ K, require reinterpretation. For $T < 30$ K, however, Li et al. find a limiting quenching constant of 500 s^{-1}. This value may be unambiguously associated with k_Q of Trp in van der Waals contact with disulfide, since thermally activated triplet–triplet energy transfer or other thermally activated processes would be insignificant at these temperatures. The value of k_Q should fall off exponentially with the distance, x, beyond van der Waals contact,

$$k_Q(x) = k_Q(0) \exp(-2x/L). \quad (27)$$

In Eq. 27, L is the effective Bohr radius. For HEWL, $x \sim$ 2 Å for the separation between Trp 63 and Cys 76–Cys 94. Assuming $L \sim$ 1 Å, k_Q is predicted to be 9 s^{-1}. The presence of a second local disulfide, Cys 64–Cys 80, with a somewhat larger x should increase k_Q to >10 s^{-1}, the value that we used in fitting the data for HLA, BLA, and HEWL. Of course, any value of $k_Q > 3$ s^{-1} produces equally good agreement. The small magnitude of $k_Q(0)$ perhaps is surprising for an electron transfer process that occurs near the barrier-free limit (20). Li et al. (6) suggested that spin dynamics may play a significant role in the electron transfer quenching mechanism, since triplet-to-singlet state interconversion of a newly formed anion–cation pair would be required in order to prevent the system from recombining to form the triplet state. In this case, the quenching rate should be enhanced by the application of an external magnetic field to accelerate triplet-to-singlet interconversion of the radical pair (29).

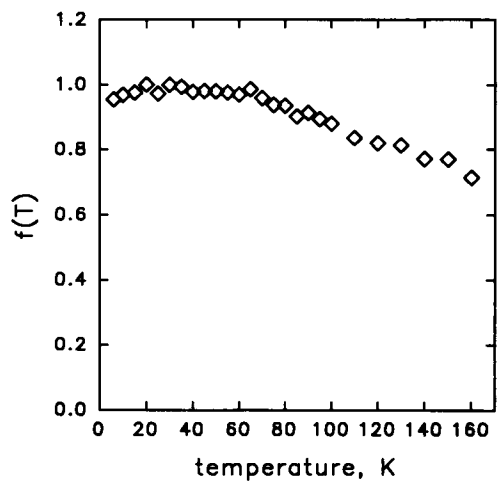

FIGURE 7 The data from GPLA, plotted on the same scale as in Figs. 4–6 for comparison. No least-squares fit was performed on this sample. GPLA was not expected to fit the physical model presented (see text), since it lacks the acceptor Trp 60 of the proposed $d \Rightarrow a$ energy transfer pair. The small temperature dependence of $[\Phi_p(T)/\Phi_f(T)]/[\Phi_p(0)/\Phi_f(0)]$ relative to the three other proteins should be noted.

TABLE 4 Output from nonlinear least-squares fit

Species	ΔE_f	k_{tr}	Norm
	cm^{-1}	s^{-1}	
HLA	97.3	1.91	0.104
BLA	143	2.66	0.217
HEWL	130	4.95	0.256

The parameters k_Q and $\Delta E_r/k$ were fixed at the values 10 s^{-1} and 800 K, respectively, for all fits. This model is not expected to fit GPLA, since it lacks the acceptor Trp at position 60. Therefore, data for this sample were not subjected to a least-squares fit. Abbreviations, see Table 1.

Triplet–triplet energy transfer is known to proceed via an exchange mechanism, following the same Dexter-type distance dependence that Li et al. suggest for the disulfide quenching event. Triplet–triplet energy transfer has been discussed by Turro (30), and seems applicable in this case: (*a*) triplet–triplet energy transfer is forbidden by a dipole–dipole (Förster) mechanism, because of very small extinction coefficients; (*b*) energy transfer would be detectable with separation distances up to 10–15 Å; (*c*) long lifetimes for the triplet states involved would mean higher probability that electronic excitation energy could be transferred. The Dexter-type exchange mechanism may be expressed by the following:

$$k_{et}(\text{exchange}) = KJ \cdot \exp(-2R_{da}/L), \qquad (28)$$

where K is a parameter related to specific orbital interactions, J is a spectral overlap integral, R_{da} is the donor–acceptor separation distance beyond van der Waals contact, and L is the average van der Waals radius for the donor and acceptor. The preexponential KJ appearing in Eq. 28 above represents an exchange integral between the donor and acceptor at van der Waals contact. A previous study of intramolecular triplet–triplet energy transfer between a ketone donor and naphthalene acceptor found $KJ \sim 2 \times 10^{15}\ s^{-1}$ and $L \sim 0.9$ Å (31). This value of KJ may be some orders of magnitude smaller for Trp–Trp energy transfer because of a smaller J. An electron spin resonance study of a single mixed crystal of naphthalene-h_8 in a matrix of naphthalene-d_8 found the exchange energy between two adjacent naphthalene molecules in van der Waals contact to be $\sim 1.5 \times 10^{11}\ s^{-1}$ (32). If we take $L = 1$ Å and $R_{da} \sim 5$ Å for the donor–acceptor pair (see below), it follows that $\exp(-2R_{da}/L) \sim 10^{-6}$. Then, if KJ is in the range 10^{11}–$10^{12}\ s^{-1}$, as suggested above, it is clear that the rate constant for barrier-free triplet–triplet energy transfer would fall into the range 10^5–$10^6\ s^{-1}$.

This model requires that the temperature-dependent energy transfer step takes place before the disulfide quenching. The observed energy barrier to forward transfer may be related to a reorganization of the solvent structure within the rigid protein matrix supporting the donor and acceptor. This reorganization appears to be quite slow in each of the proteins, as evidenced by the values of $\sim$2–5 s^{-1} for the k_{tr} parameter obtained from fitting the data (Table 4). Once this reorganization has proceeded, we believe the ensuing energy transfer to be rapid as outlined above. If our estimate of $k_Q \sim 10\ s^{-1}$ is compared with k_{tr}, these results suggest that reverse transfer before quenching has little probability at the temperatures used in this study.

As discussed above, Figs. 4–6 and the data in Table 4 show that the model fits the data from HLA better than those from BLA or HEWL, as evidenced by the smaller norm of the fit. This is not unexpected, since HLA, containing three Trps, is the simplest system studied that contains the $d \Rightarrow a$ pair. BLA and HEWL both show similar temperature dependence and poorer goodness of fit. This suggests that Trp 26 in BLA (or Trp 28 in HEWL), which is absent in HLA, may contribute to the total temperature-dependent luminescence quenching observed in these two systems. Fig. 7 reveals only a small temperature dependence of the quantum yield ratio for GPLA, which is missing the acceptor Trp 60 in the proposed $d \Rightarrow a$ pair. GPLA contains Trp 26, however, further suggesting that this Trp may be involved in some minor temperature-dependent triplet quenching mechanism. The smaller temperature dependence also may be the result of less efficient energy transfer from Trp 104 to another acceptor, Trp 118, for instance, that should be quenched efficiently by the nearby disulfide, Cys 28–Cys 111. The small degree of thermally activated phosphorescence quenching exhibited by GPLA, in contrast to the other proteins studied, provides critical supporting evidence for the essential correctness of the quenching model used. We conclude, therefore, that the GPLA data further confirm the assignment of Trp 104 $\Rightarrow$ Trp 60 as the major $d \Rightarrow a$ pair in the α-lactalbumins and Trp 108 $\Rightarrow$ Trp 63 as the corresponding $d \Rightarrow a$ pair in HEWL.

Fig. 8, *a* and *b*, shows a comparison of the crystal structures of HEWL and baboon α-lactalbumin, the coordinates for both having been taken from the Brookhaven Protein Data Bank (13, 14) and displayed via the molecular modeling program InsightII version 2.1.0 (Biosym Technologies, Inc., San Diego, CA). The HEWL structure (Fig. 8 *a*) reveals that the donor, Trp 108, is very nearly parallel planar and separated by $\sim$8.5 Å from the acceptor, Trp 63. Similarly, the baboon α-lactalbumin structure (Fig. 8 *b*) shows a donor–acceptor separation of $\sim$9.1 Å. As stated earlier, the relative orientation observed in the structure of baboon α-lactalbumin is assumed to occur also in HLA, and should be very similar among all α-lactalbumins. Such a parallel planar arrangement would be considered very favorable for triplet–triplet energy transfer, as the overlap of the two indole π-systems would be greatest along an out-of-plane axis.

Conclusions

In this work, we have presented results showing temperature-dependent phosphorescence emission originating primarily from Trp 108 in HEWL, and its structural equivalent, Trp 104, in the α-lactalbumins from bovine, human, and guinea pig. A thermally activated triplet–triplet energy transfer process was proposed to occur in HLA and BLA from the Trp 104 donor (and from Trp 108 in HEWL) to the Trp 60 acceptor (Trp 63 in HEWL), where the excitation energy is quenched directly by a nearby disulfide. A physical model was presented, based on a two-level system, that accounts for the observed temperature dependence, with the best agreement found for the simplest system, HLA. We found

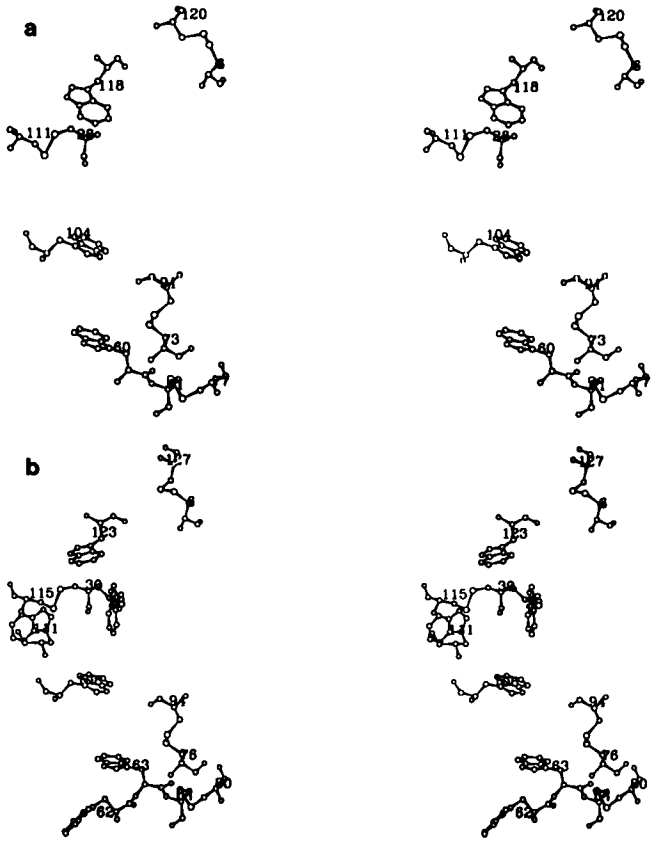

FIGURE 8 A depiction of the Trps and disulfide bonds present in baboon α-lactalbumin (a) and in HEWL (b). These coordinates were taken from Brookhaven Protein Data Bank entries referenced in the text and displayed via InsightII software. The Trp 104–Trp 60 separation in a is 9.1 Å, and the Trp 108–Trp 63 separation in b is 8.5 Å.

that the energy barrier for forward transfer ranges between $\sim$100 and $\sim$150 cm^{-1}, while the barrier for reverse transfer probably occurs in the range $\sim$100–600 cm^{-1}. This barrier creates a trap for the transferred energy at the quenching site. The rate constant for forward and reverse energy transfer has a high-temperature limit of $\sim$2–5 s^{-1}, which we believe is controlled by a very slow reorganizational motion of the rigid matrix in the vicinity of the $d \Rightarrow a$ pair. The extrinsic quenching constant k_Q was assumed to have a value of $\sim$10 s^{-1}, and other measurements on long-chain snake neurotoxins (5, 6) suggest that it has little temperature dependence. This value is comparable with that derived from low-temperature measurements of Li et al. on model systems (6).

We thank Dr. Marvin Thompson for providing a purified sample of guinea pig α-lactalbumin.

This work was partially supported by a grant from the National Institutes of Health (ES-02662).

Received for publication 13 October 1992 and in final form 4 January 1993.

REFERENCES

1. Churchich, J. E. 1966. Tryptophan residues in native and reoxidized muramidase: luminescence properties. *Biochim. Biophys. Acta.* 120:406–412.
2. Cowgill, R. W. 1967. Fluorescence and protein structure. XI. Fluorescence quenching by disulfide and sulfhydryl groups. *Biochim. Biophys. Acta.* 140:37–44.
3. Longworth, J. W. 1971. Luminescence of polypeptides and proteins. *In* Excited States of Proteins and Nucleic Acids. R. F. Steiner and I. Weinryb, editors. Plenum Publishing Corp., New York. 319–484.
4. von Schütz, J. U., J. Zuclich, and A. H. Maki. 1974. Resolution of tryptophan phosphorescence from multiple sites in proteins using optical detection of magnetic resonance. *J. Am. Chem. Soc.* 96:714–718.
5. Schlyer, B. D., E. Lau, and A. H. Maki. 1992. A comparative investigation of snake venom neurotoxins and their triplet-state tryptophan–disulfide interactions using phosphorescence and optically detected magnetic resonance. *Biochemistry.* 31:4375–4383.
6. Li, Z., A. Bruce, and W. C. Galley. 1992. Temperature dependence of the disulfide perturbation to the triplet state of tryptophan. *Biophys. J.* 61:1364–1371.
7. Berliner, L. J., and J. D. Johnson. 1988. α-lactalbumin and calmodulin. *In* Calcium-Binding Proteins. Biological Functions. Vol. II. M. P. Thompson, editor. CRC Press, Inc., Boca Raton, FL. 79–116.
8. Sommers, P. B., and M. J. Kronman. 1980. Comparative fluorescence properties of bovine, goat, human, and guinea pig α-lactalbumin. Characterization of the environments of individual tryptophan residues in partially folded conformers. *Biophys. Chem.* 11:217–232.
9. Swadesh, J. K., P. W. Mui, and H. A. Scheraga. 1987. Thermodynamics of the quenching of tyrosyl fluorescence by dithiothreitol. *Biochemistry.* 26:5761–5769.
10. Sanyal, G., E. Kim, F. M. Thompson, and E. K. Brady. 1989. Static quenching of tryptophan fluorescence by oxidized dithiothreitol. *Biochem. Biophys. Res. Commun.* 165:772–781.
11. Bent, D. V., and E. Hayon. 1975. Excited state chemistry of aromatic acids and related peptides. III. Tryptophan. *J. Am. Chem. Soc.* 97:2612–2619.
12. Blake, C. C. F., D. F. Koenig, G. A. Mair, A. C. T. North, D. C. Phillips, and V. R. Sarma. 1965. Structure of hen egg-white lysozyme. A three-dimensional Fourier synthesis at 2 Å resolution. *Nature (Lond.).* 206:757–761.
13. Kurachi, K., L. C. Sieker, and L. H. Jensen. 1976. Structures of triclinic mono- and di-*N*-acetylglucosamine:lysozyme complexes—a crystallographic study. *J. Mol. Biol.* 101:11–24.
14. Acharya, K. R., D. I. Stuart, N. P. C. Walker, M. Lewis, and D. C. Phillips. 1989. Refined structure of baboon α-lactalbumin at 1.7 Å resolution. Comparison with C-type lysozyme. *J. Mol. Biol.* 208:99–127.
15. Imoto, T., L. S. Forster, J. A. Rupley, and F. Tanaka. 1971. Fluorescence of lysozyme: emissions from tryptophan residues 62 and 108 and energy migration. *Proc. Natl. Acad. Sci. USA.* 69:1151–1155.
16. Rousslang, K. W., J. M. Thomasson, J. B. Alexander Ross, and A. L. Kwiram. 1979. Triplet state of tryptophan in proteins. 2. Differentiation between tryptophan residues 62 and 108 in lysozyme. *Biochemistry.* 18:2296–2300.
17. Li, Z., and W. C. Galley. 1989. Evidence for ligand-induced conformational changes in proteins from phosphorescence spectroscopy. *Biophys. J.* 56:353–360.

18. Li, Z., W. E. Lee, and W. C. Galley. 1989. Distance dependence of the tryptophan-disulfide interaction at the triplet level from pulsed phosphorescence studies on a model system. *Biophys. J.* 56:361–367.

19. Tamaki, T. 1981. Sensitization of the phosphorescence of indole through intramolecular energy transfer from the triplet state of covalently linked acetophenone in rigid media at 77 K. *Photochem. Photobiol.* 33:31–34.

20. Marcus, R. A., and N. Sutin. 1985. Electron transfers in chemistry and biology. *Biochim. Biophys. Acta.* 811:265–322.

21. Kronman, M. J., S. K. Sinha, and K. Brew. 1981. Characteristics of the binding of Ca^{2+} and other divalent metal ions to bovine α-lactalbumin. *J. Biol. Chem.* 256:8582–8587.

22. Brenner, H. C., and V. Kolubayev. 1988. ODMR in ethylene glycol–aqueous buffer mixtures: enhancement of triplet spin lattice relaxation at high aqueous concentrations. *J. Lumin.* 39:251–257.

23. Miller, J. N., and L. A. King. 1975. The low-temperature luminescence properties of bovine alpha-lactalbumin. *Biochim. Biophys. Acta.* 393:435–445.

24. Hall, L. H., and M. A. El-Sayed. 1975. Temperature dependence of the spin-lattice relaxation rates in the triplet state of pyrazine at low temperatures. *Chem. Phys.* 8:272–288.

25. Purkey, R. M., and W. C. Galley. 1970. Phosphorescence studies of environmental heterogeneity for tryptophyl residues in proteins. *Biochemistry.* 9:3569–3575.

26. Davis, J. M., and A. H. Maki. 1984. Comparative phosphorescence and optically detected magnetic resonance studies of pig and yeast glyceraldehyde-3-phosphate dehydrogenase. *Biochemistry.* 23:6249–6256.

27. Tsao, D. H. H., and A. H. Maki. 1991. Optically detected magnetic resonance study of the interaction of an As(III) derivative of cacodylic acid with *Eco* RI methyl transferase. *Biochemistry.* 30:4565–4572.

28. Lam, W.-C., D. H. H. Tsao, A. H. Maki, K. A. Maegley, and N. O. Reich. 1992. Spectroscopic studies of arsenic (III) binding to *Escherichia coli* RI methyl transferase and to two mutants, C223S and W183F. *Biochemistry.* 31:10438–10442.

29. Frankevich, E. L., and S. I. Kubarev. 1982. Spectroscopy of reaction-yield detected magnetic resonance. *In* Triplet State ODMR Spectroscopy. R. H. Clarke, editor. Wiley-Interscience, New York. 137–183.

30. Turro, N. J. 1967. Modern Molecular Photochemistry. W. A. Benjamin, San Francisco, CA. 628 pp.

31. Maki, A. H., J. G. Weers, E. F. Hilinski, S. V. Milton, and P. M. Rentzepis. 1984. Time-resolved spectroscopy of intramolecular energy transfer in a rigid spiran. *J. Chem. Phys.* 80:2288–2297.

32. Schwoerer, M., and H. C. Wolf. 1967. ESR investigations of naphthalene-d_8:naphthalene-h_8 mixed crystals. *In* The Triplet State. A. B. Zahlan, G. M. Androes, H. F. Hameka, F. W. Heineken, C. A. Hutchison, Jr., G. W. Robinson, and J. H. van der Waals, editors. Cambridge University Press, London. 133–140.